NOVEL SCHEME OF AMORPHOUS/CRYSTALLINE SILICON HETEROJUNCTION SOLAR CELL

M. Tucci[1], L. Serenelli[1], E. Salza[1],
S. De Iuliis[2], L. J. Geerligs [2],
G. de Cesare[3], D. Caputo[3], M. Ceccarelli[3]

[1] ENEA Research Center Casaccia Via Anguillarese, 301, 00123 Roma Italy
Phone: +39(06)30484095, Fax : +39(06)30486405, e-mail: mario.tucci@casaccia.enea.it
[2] ECN Solar Energy, P.O. Box 1 NL-1755 ZG Petten, The Netherlands
[3] Department of Electronic Engineering University of Rome "La Sapienza", via Eudossiana, 18, 00184 Roma, Italy

ABSTRACT**:** In this paper we investigate in detail how the heterostructure concept can be implemented in an interdigitated back contact solar cell, in which both the emitters are formed on the back side of the c-Si wafer by amorphous/crystalline silicon heterostructure, and at the same time the grid-less front surface is passivated by a double layer of amorphous silicon and silicon nitride, which also provides an anti-reflection coating. The entire process, held at temperature below 300 °C, is photolithography-free, using a metallic self-aligned mask to create the interdigitated pattern, and we show that the alignment is feasible. An open-circuit voltage of 687 mV has been measured on a p-type monocrystalline silicon wafer. The mask-assisted deposition process does not influence the uniformity of the deposited amorphous silicon layers. Photocurrent limits factor has been investigated with the aid of one-dimensional modeling and quantum efficiency measurements. On the other hand several technological aspects that limit the fill factor and the short circuit current density still need improvements.
Keywords: heterojunction, back contact.

1 INTRODUCTION

Reducing the overall photovoltaic module and system costs is the challenge to make the energy production from PV competitive. This could be efficiently done increasing the silicon based solar cell efficiency, even though these savings are offset by the more complicated processing required [1]. A way to increase PV conversion efficiency is represented by rear-junction, back-contact, design interdigitated, (IBC) solar cell able to collect photogenerated carriers entirely from the rear of the cell. The advantages of this structure include no contact grid shading on the sunward side and use of a thin substrate [2]. Another useful concept for increasing c-Si based solar cells is the one adopted by Sanyo's HIT structure in which high-quality intrinsic a-Si:H layers allow an excellent surface passivation of c-Si surface, resulting in high efficiency, especially a high open circuit voltage (V_{oc}): almost 730 mV, has been reached [3]. Moreover the temperature coefficient of HIT cells is better than conventional c-Si solar cells and results in a higher output power at high temperatures [4]. Indeed the low-temperature processes (< 200 ºC) result in an advantage for thinner c-Si wafers. Finally the implementation of amorphous / crystalline silicon (a-Si:H / c-Si) heterojunction as solar cell concept has the capability of reaching efficiencies up to 25% [5, 6]. Here we show how the heterostructure technology can have a chance in the challenge of the IBC solar cells. We present an innovative design of the solar cell in which both the emitter and the back contact are formed by (a-Si:H/c-Si) heterostructure and placed at the rear side, and the grid-less front surface is passivated by a double layer of amorphous silicon and silicon nitride, which also provides anti-reflection coating [7]. We have named this device BEHIND cell (Back Enhanced Heterostructure with INterDigitated contacts cell). We show preliminary results on textured p-type monocrystalline silicon wafers: We investigate and discuss in detail the technological issues, needed to develop our process technology, and analyze the results by individuating way of improvements with the aid of simulations.

2 EXPERIMENTAL DETAILS

BEHIND solar cells are fabricated starting from 4 inch diameter, 250 µm thick, <100> oriented, 0.5 Ωcm p-type, one side polished FZ silicon wafers, on which we have obtained four 6.25 cm^2 area devices. We have performed a front surface alkaline texturization, while we have chosen the wafer polished side as the back side of the cell. All a-Si:H deposition processes has been performed in a 13.56 MHz direct Plasma Enhanced Chemical Vapour Deposition (PECVD) system equipped with three chamber, each dedicated to a particular doping type. On the whole polished side of the wafer, after a standard RCA cleaning and HF dip, 5 nm thick intrinsic a-Si:H buffer layer and subsequent 15 nm thick n-type doped a-Si:H have been deposited. After 1% HF bath, we have deposited on the sunward side 5 nm and 70 nm of a-Si:H and SiN_x respectively as passivation/antireflection coating. We have chosen a a-Si:H/SiN_x double layer instead of single SiN_x layer, since it has been demonstrated higher passivation properties with respect to the SiN_x produced by the same system [7]. In turn we loose part of the blue sun-spectrum due to the a-Si:H absorption of the high energy photons. To form the p-type contact we have fabricated a particular metal mask scribing a comb shape grid, with the aid of a Nd-YAG laser at a wavelength of 1064 nm, on 100 µm thick Molybdenum foil. This mask is opportunely fixed on the rear side of wafer by a particular designed holder. To remove the n-type a-Si:H portion under the p-type contact a dry etching procedure using NF_3 gas has been performed, using settings defined on the base of previous experience [8], which allows to avoid damages and fluorine radicals contaminations at the silicon surface. In particular 30 s has been estimated sufficient to etch about the 15 nm thick a-Si:H n-layer. To ensure an isolation between the n-type doped a-Si:H edges and the p-type doped a-Si:H areas we have subsequently deposited, in the patterned region, a very thin intrinsic buffer layer of about 5 nm prior to grow the 15 nm p-type a-Si:H film. Keeping the metallic mask still held on the sample, we have then evaporated 2 µm of Al on the p-type a-Si:H to

form the base contact. Finally we have rotated the mask in the holder of 180° and evaporated 2 μm thick Ag contact on the n-type a-Si:H layer. We remark that the mask alignment is not critical since the emitter width is at least three times wider than the base contact. We have dimensioned the distance between two adjacent fingers of the interdigitated combs supposing a diffusion length of minority photogenerated carriers in the order of 400 μm. Schematic diagram of the BEHIND solar cell process is shown in Figure 1. The process parameters used in PECVD system are summarized in Table I.

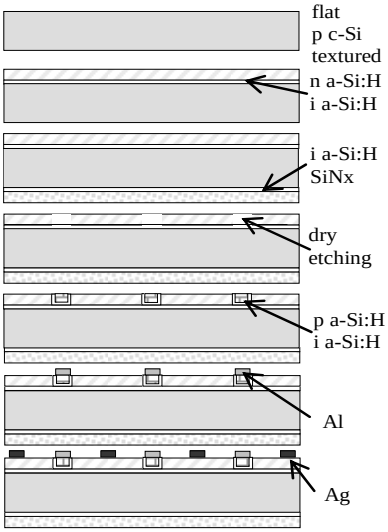

Figure 1: Schematic diagram of BEHIND cell process.

Table I: Deposition parameters of BEHIND cell

Process Step	RF power (mW/cm^2)	Temperature (°C)	Pressure (mTorr)	Gas flows
i a-Si:H back layer	28	300	300	40 sccm SiH_4
n a-Si:H back layer	28	300	300	10 sccm PH_3/SiH_4 5%; 40 sccm SiH_4
i a-Si:H front layer	36	250	750	120 sccm of 5% SiH_4 diluted in Ar
SiN_x front layer	260	250	750	1.66 as NH_3/SiH_4 gas flows ratio
dry etching	400	25	50	48 sccm NF_3
p a-Si:H layer	28	300	300	6 sccm of B_2H_6; 40 sccm SiH_4

At this stage the BEHIND cells have been characterized in terms of current-voltage (IV), both in dark and AM1.5G conditions, reflectance and Quantum Efficiency (IQE: internal quantum efficiency; EQE: external quantum efficiency). To reduce the series resistance we have irradiated, by a Q-switched Nd-YAG laser, the Al contact following the comb pattern by a PC controlled XY stage able to move the substrate at 10 mm/s under the beam. The used laser settings (wavelength at 1064 nm, mode TEM00, power 320 mW, repetition rate 1KHz) have been chosen on the base of previous work [9].

3 RESULTS AND DISCUSSION

The IV characteristic in this study have been measured at room temperature under 100 mW/cm^2 AM1.5G. They are shown in the Figure 2 as symbols.

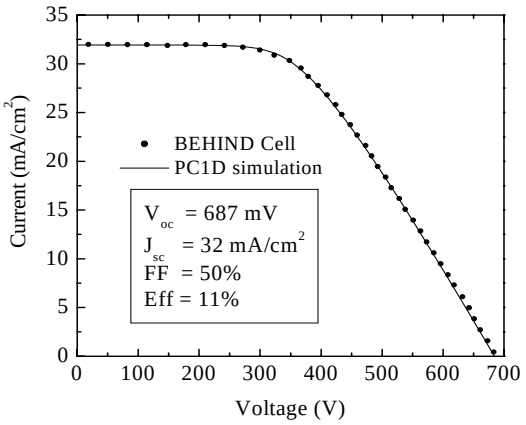

Figure 2: IV measurements and photovoltaic parameters under AM1.5G condition: experimental data (symbols) and PC1D simulations (lines).

The feasibility of alignment and the unaffecting on the uniformity of the deposited amorphous silicon layers by the mask-assisted deposition process is confirmed by the 687 mV as open circuit voltage (V_{oc}) value, which also depends on the isolation of the regions where the doped layers can overlap. We remark that at the end of fabrication process the cell photocurrent has been completely dominated by a very high series resistance. A laser treatment over the Al contacts can overcome this problem, knowing that this treatment is able to promote, in the right conditions [9], Al and B (being within the p-type a-Si:H material) diffusion into the crystalline base, thus producing a less resistive contact, even if in a narrow region. On the other hand, the short circuit current (J_{sc}) is limited to 32 mA/cm^2 even though the sunward surface is not shaded at all by any metal grid. The integration of EQE data over the sun spectrum confirms this data. A detailed view of IQE, EQE and reflectance measurements is reported in Figure 3 as symbols.

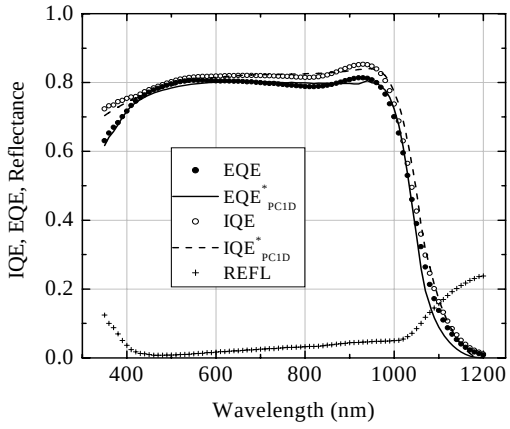

Figure 3: IQE, EQE, Reflectance of the BEHIND cell: experimental data (symbols) and PC1D simulations (lines).

As mentioned, the J_{sc} value is less than the expected one due to both optical and recombination losses. Theoretically the photocurrent should be higher than measured, due to the BEHIND design. Indeed the photocurrent is mainly due to electron diffusion in the p-type doped crystalline base, plus a contribute of depletion. Since the position of the p-n heterojunction is

on the backside, we could expect to have overcomed the problem of emitter absorption, that still affects the n-type a-Si:H/p-type c-Si heterostructure solar cell, due to low band gap of the n-type a-Si:H layer that does not exceed 1.65 eV [10]. To obtain high J_{sc} we have to focus on diffusion length, L_d, and surface recombination velocity, $S_{n,p}$., exploring the effect of both parameters on the basis of EQE experimental data. We have compared it with a PC1D [11] simulation, in which we have simplified our BEHIND cell into one dimensional crystalline based solar cell having a back thin n-type a-Si:H emitter layer. A detailed description of parameters adopted in the simulation is reported in Table II.

Table II Parameters used in PC1D simulation.

c-Si parameters	Values
thickness (μm)	250
mobility μ_n , μ_p (cm^2/Vs)	1417, 470
bandgap (eV)	1.124
intrinsic concentration n_i (cm^{-3})	1^x10^{10}
absorption coefficient (model)	[12]
p-type doping (cm^{-3})	3.2^x10^{16}
diffusion lenght L_d (μm)	500
front surface recomb. S_n,S_p (cm/s)	80, 80
rear surface recomb. S_n,S_p (cm/s)	1^x10^6, 1^x10^6
a-S:H parameters	
thickness (μm)	0.015
mobility μ_n , μ_p (cm^2/Vs)	1, 0.1
bandgap (eV)	1.65
intrinsic concentration n_i (cm^{-3})	1^x10^7
absorption coefficient (model)	[13]
μτ (cm^2/V)	1^x10^{-12}
n-type doping (cm^{-3})	5^x10^{17}

Those parameters have been fixed on the based of both c-Si and a-Si:H properties and on geometrical characteristic of the cell. Taking also into account the measured reflectance profile, reported in Figure 3 as symbols, we have obtained a good agreement between experimental data and simulation model. Only the contribution of higher energy photons is different, since the simulation does not account for the passivation/antireflection coating absorption. So at the end of EQE simulation, those data have been reduced by the a-Si:H thin layer (d = 3 nm) absorption as follows:

$$EQE^{*}_{PC1D}(\lambda) = EQE_{PC1D}(\lambda) \cdot e^{-\alpha_{a-Si:H}(\lambda)\cdot d} \quad (1)$$

where: $\alpha_{a\text{-}Si:H}$ is the a-Si:H absorption coefficient and EQE_{PC1D} is the EQE data as calculated by PC1D. The modeling suggest that with $S_{n,p}$ down to 10 cm/s and L_d up to 1 mm or wafer thickness down to 170 μm, it would be possible to reach the maximum IQE values of this kind of device. Lower $S_{n,p}$ and longer L_d can be reached having more care in substrate preparation, as demonstrated by the same group in other work [7].

Since the cell rear side is not homogeneous in term of depletion depth, the QE varies depending on the monochromatic spotlight dimension and position with respect to the fingers of the rear contacts. For this reason we have performed different measurements, using a focused spotlight having dimension comparable to that of single finger contact, reported in Figure 4. When a single n-type finger is illuminated a hump in the EQE data appears in the spectral region ranging from 900 nm and 950 nm, due to the depletion region that enhance the photogeneration collection toward the n-type a-Si:H layer. In turn, when a single p-type finger is illuminated, the EQE profile results smooth over the entire spectrum because of lack of electric field close to the p-type c-Si/p-type a-Si:H/Al contact.

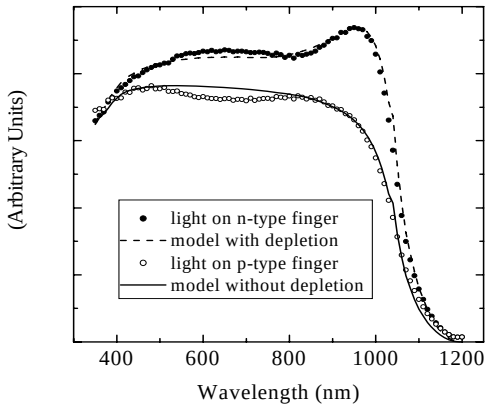

Figure 4: Comparison of normalised photocurrent, measured using narrow spotlight size shined on different doped fingers of the BEHIND cell.

The photocurrent contributions of the different cell regions can be discriminated by using the following expression for generation we have modeled:

$$G(\lambda) = e^{-\alpha_{a-Si:H}(\lambda)\cdot d}\left[1 - \frac{e^{-\alpha_{c-Si}(\lambda)\cdot t}}{1+\alpha_{c-Si}(\lambda)\cdot L_D} + \right. \quad (2)$$
$$\left. + e^{-\alpha_{c-Si}(\lambda)\cdot(t-W)}\cdot\left(1 - e^{-\alpha_{c-Si}(\lambda)\cdot W}\right)\right]$$

where t is the wafer thickness, $\alpha_{c\text{-}Si}$ is the c-Si absorption coefficient, and W is the depletion depth. The contribute of the intrinsic a-Si:H can be neglected keeping in mind that the c-Si bulk thickness blind it. Taking into account only the contribution to the photocurrent given by a single p-type finger illuminated, reported in Figure 4, the generation can be evaluated only with the left term of (2), while when a single n-type finger is illuminated the contribute of the depletion depth, described in the right term of (2), becomes more evident than in case of EQE measurements obtained by a monochromatic spotlight area larger than several finger contacts. With the same set of parameters reported in Table II we have also fitted the IV characteristic under sunlight exposure, reported in Figure 2 as continuous line. The low Fill Factor has been considered in terms of an addition of series resistance, to simulate the effect of low lateral conductivity of the n-type a-Si:H emitter. This problem mainly arises from the p-type c-Si / i a-Si:H / p-type a-Si:H contact in which the carrier transport is determined by tunneling mechanism, due to the relevant band offset between the two valence band of p-type c-Si and p-type a-Si:H [14]. In our samples the necessity to avoid shunts between the two amorphous doped layers, has induced to deposit thick buffer layers, so the thicknesses of amorphous layers could be thicker than expected. The series resistance can be lowered reducing the thicknesses of both p-type and intrinsic a-Si:H layers and introducing a method to increase the conductivity of the p-type a-Si:H layer as well as the n-type layer conductivity, forming a thin CrSi layer on it, that can be really useful also on the n-type amorphous emitter [15]. Moreover the density of fingers should be incremented.

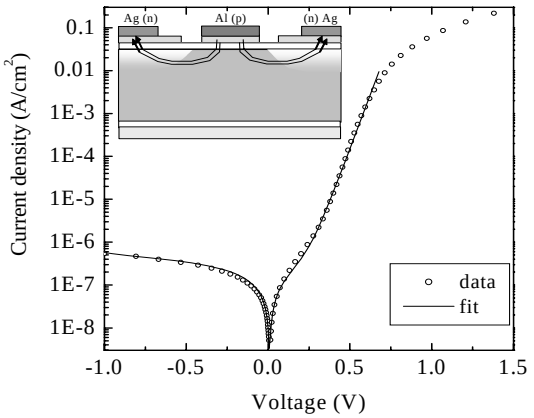

Figure 5: IV characteristic at room temperature and dark conditions. In the inset how to the dark current flows between rear contacts.

To exploit the V_{oc} value we have measured IV characteristic at room temperature and dark conditions. In the inset of Figure 4 is depicted the path of dark current, which mainly flows between the fingers shaped back contacts in a region almost depleted. To extract Informations about the recombination in the depletion region, within the crystalline close to the heterojunction, are extractable adopting the following detailed expression to describe the dark IV curve:

$$I(V) = I_0\left(e^{\frac{V}{n_1 V_T}} - 1\right) + I_r e^{\frac{V}{n_2 V_T}} - I_g\left(\frac{1}{1-(|V|/BV)^{n_3}}\right) \quad (3)$$

where I_0 is the diode reverse saturation current; I_r, I_g are the recombination and thermal generation currents in the depletion region respectively; BV is the breakdown voltage; n_1, n_2, n_3 are the ideality factors and V_T is the thermal equivalent voltage. By fitting procedure, reported in Figure 5 as line, we have obtained the values reported in Table 3.

Table III Parameters used to fit the IV dark data.

Parameters	Values
I_0 reverse current (A/cm^2)	$1.3\ 10^{-9}$
I_r recombination in the depletion region (A/cm^2)	$4.5\ 10^{-7}$
I_g thermal generation in the depletion region (A/cm^2)	$4.6\ 10^{-7}$
n_1 ideality factor	1.65
n_2 ideality factor	8
n_3 ideality factor	3
BV breakdown voltage (V)	1.6

In this model we have neglected the current flowing through the amorphous intrinsic insulator between the two rear contacts, because both its poor conductivity (at least $10^{-11}\ \Omega^{-1}cm^{-1}$) and its thin thickness (10 nm). Also the depletion inside the n-type a-Si:H has been neglected, due to its defect density and dopant concentration [10]. At high current injection level the transport mechanism is dominated by the series resistance, as already seen in the lighted IV curve, not described by the equation (3). From the latter analysis we can conclude that the recombination mechanism limits the V_{oc}. However the built-in potential, arising from the c-Si/a-Si:H heterojunction, still remains sufficiently high to determine a Voc value of 687 mV.

4 CONCLUSIONS

In this paper we have shown the BEHIND cell as an innovative design of the a-Si:H/c-Si heterostructure solar cell, where both the emitter and the back contact are formed and placed on the backside by amorphous/crystalline silicon heterostructure. The grid-less front surface has been passivated by a double layer of amorphous silicon and silicon nitride (a-Si:H/SiN_x), which also provides anti-reflection coating. The mask-assisted deposition of a-Si:H layer is feasible and only one metallic mask is used in the entire fabrication process. We have analysed the generation mechanism of different regions of the back contacts. With the aid of a PC1D model we have deduced the properties of transport and recombination and we have addressed the way for future improvements. Anyway a V_{oc} of 687 mV has been reached, that can be considered a good starting point to continue to develop this low temperature process useful to reduce the PV manufacturing cost.

REFERENCES

[1] W.P. Mulligan, D.H. Rose, M.J. Cudzinovic, D.M. De Ceuster, K.R. McIntosh, D.D. Smith, and R.M. Swanson, Proc. of 19th European Photovoltaic Solar Energy Conference (2004) 387.

[2] R.M. Swanson, Proc. of the 31st IEEE PVSEC, Lake Buena Vista, 2005; 889–894.

[3] W. P. Mulligan, M. A. Carandang, M. Dawson, D. M. De Ceuster, C. N. Stone, and R. M. Swanson, Proc. of XXI European Photovoltaic Solar Energy Conference (2006) 1301.

[4] M. Taguchi, K. Kawamoto, S. Tsuge, T. Baba, H. Sakata, M. Morizane, K. Uchihashi, N. Nakamura, S. Kiyama and O. Oota, Prog. Photovolt: Res. Appl. 8 (2000) 503.

[5] E. Maruyama, A. Terakawa, M. Taguchi, Y. Yoshimine, D. Ide, T. Baba, M. Shima, H. Sakata, and M. Tanaka, Proc. of 4th World Conference Photovoltaic Energy Conversion, (2006) 1455.

[6] M. Taguchi, A. Terakawa, E. Maruyama and M. Tanaka, Prog. Photovolt: Res. Appl. 3 (2005) 481.

[7] M. Tucci, L. Serenelli, S. De Iuliis, M. Izzi in press on Thin solid Film 515 (2007) 7625.

[8] M. Tucci, L. Serenelli, S. De Iuliis, E. Salza, L. Pirozzi; Proc. of 21st European Photovoltaic Solar Energy Conference (2006) 1250.

[9] L. Kreinin, N. Bordin, J. Broder, N. Eisenberg, M. Tucci, E. Talgorn, S. De Iuliis, L. Serenelli, M. Izzi, E. Salza, L. Pirozzi; Proc. of 21st European Photovoltaic Solar Energy Conference (2006) 855.

[10] M. Tucci, G. de Cesare, J. of Non-Cryst. Solids 338 (2004) 663.

[11] PC1D version 5.3 P.A. Basore, D.A. Clugston University of New South Wales (1998).

[12] M.A. Green, M.J. Keevers Progress in Photov. res. & appl. 3 (1995) 189.

[13] ED. Palik. Handbook of optical constants of solids New York Academic Press (1985) 571.

[14] Mario Tucci , L Serenelli , S De Iuliis, D Caputo, A Nascetti, G de Cesare. Proceeding of XXI European Photovoltaic Solar Energy Conference Dresden (2006) 902.

[15] D. Caputo, G. de Cesare, A. Nascetti, M. Tucci. J. of Non-Cryst. Solids 352 (2006) 1818.